

DOI:10.11918/201905049

欠驱动 USV 神经网络自适应轨迹跟踪控制

张成举, 王聪, 曹伟, 王金强

(哈尔滨工业大学 航天学院, 哈尔滨 150001)

摘要:为解决欠驱动 USV 系统在模型不确定性和未知海流干扰下的水平面轨迹跟踪问题,基于反步法与自适应技术,提出一种非线性鲁棒轨迹跟踪控制策略.针对欠驱动 USV 参数不确定问题,运用神经网络自适应方法对欠驱动 USV 系统未知函数进行估计和逼近;然后,运用动态面方法获取虚拟变量的导数,不仅控制律结构简单,易于工程实现,而且有效地减小了传统反步法中虚拟变量直接求导的复杂性;针对未知时变海流的干扰,设计了一种指数收敛海流观测器,有效估计未知缓慢时变海流速度;其次,基于李雅普诺夫理论证明了所设计的控制器能够保证运动轨迹收敛于期望值,并且保证了该轨迹跟踪闭环控制系统所有信号最终一致有界;最后,在控制输入受限条件下,为检验该控制器的跟踪性能,选取圆轨迹作为参考轨迹,仿真实验表明,该控制器能够有效地实现预期轨迹,神经网络自适应方法对系统未知函数可有效估计和逼近,对未知时变海流干扰具有较强的鲁棒性,轨迹跟踪误差和速度跟踪误差均收敛到零附近的一个邻域内,从而验证了所提出控制器的有效性.

关键词: 欠驱动 USV; 轨迹跟踪; 反步法; 神经网络自适应; 海流观测器

中图分类号: TP273

文献标志码: A

文章编号: 0367-6234(2020)12-0001-07

Adaptive neural network trajectory tracking control for underactuated unmanned surface vehicle

ZHANG Chengju, WANG Cong, CAO Wei, WANG Jinqiang

(School of Astronautics, Harbin Institute of Technology, Harbin 150001, China)

Abstract: To deal with the problems of horizontal trajectory tracking control of underactuated unmanned surface vehicle (USV) in the presence of model uncertainties and unknown ocean currents, a robust nonlinear trajectory tracking controller for underactuated USV was proposed based on the backstepping method and adaptive technique. For the model uncertainties of underactuated USV, the adaptive neural network technique was employed to estimate and compensate the unknown model uncertainties. Then, the derivatives of virtual control variables were obtained by dynamic surface control method. The control law was simple in structure and easy to be realized in engineering, and it greatly reduced the complexities of the traditional backstepping method. For the disturbances of unknown time-varying currents, an observer was designed to estimate the velocity of unknown time-varying currents. Next, based on Lyapunov's direct method, it was proved that the designed controller could ensure that the motion trajectory converged to the expected value, and that all signals of the trajectory tracking closed-loop control system were finally uniformly bounded. Lastly, under the condition of limited control input, in order to verify the tracking performance of the controller, the circular trajectory was selected as the reference trajectory. Simulations were carried out and results show that the controller could accurately track the desired trajectory and had strong robustness for model uncertainties and unknown time-varying currents. In addition, the unknown functions of the system were effectively estimated and compensated by adaptive neural network technique, which verified the effectiveness of the proposed tracking control scheme.

Keywords: underactuated USV; trajectory tracking; backstepping; adaptive neural network; ocean observer

欠驱动 USV 是一种新兴的水面无人舰艇,可实现海洋环境观测、资源勘查、水面运载等海洋作业;但是由于大多 USV 为复杂的欠驱动系统,各自由度之间存在较大的非线性耦合,给 USV 的运动控制带

来了较大困难;另外,USV 易受到恶劣海洋环境的影响,难以获得动力学参数,从而造成了欠驱动 USV 难以实现轨迹跟踪的难题.针对欠驱动 USV 跟踪问题,沈智鹏等^[1]通过设计神经网络观测器来获得船舶速度,仿真结果验证了该观测器的有效性,但是并未考虑未知缓慢时变海流干扰问题;杜佳璐等^[2]通过采用自适应律来估计外部干扰,提高了船舶定位精度;张天平等^[3]采用神经网络逼近系统中不确定函数,经过仿真验证了该控制算法的有效性.

收稿日期: 2019-05-08

基金项目: 国家自然科学基金(11672094)

作者简介: 张成举(1993—),男,博士研究生;

王聪(1966—),男,教授,博士生导师

通信作者: 王聪,alanwang@hit.edu.cn

廖煜雷等^[4]采用滑模控制补偿外界干扰,经仿真验证,该控制系统具有较好的鲁棒性,但是该控制方法并未考虑难以获得准确水动力系数问题;王金强等^[5]通过设计自适应律补偿难以测定的水动力系数,经仿真验证了该控制系统的有效性,但是该方法只是针对位置跟踪问题;Teek 等^[6]采用高增益观测器获得难以测定的船舶速度,经过仿真验证了该控制器的有效性;Shojaei^[7]将神经网络自适应方法运用到船舶编队方面,经过仿真验证了该方法的鲁棒性;Wang 等^[8]运用 RBF 神经网络自适应方法逼近不确定函数,通过仿真验证了该控制器的稳定性与鲁棒性,该方法仍然未考虑未知海流干扰影响;Pan 等^[9]通过设计神经网络动态模型的方法获取虚拟变量的导数,运用级联控制方法验证了该控制系统的稳定性;Wang 等^[10]采用自适应动态面方法解决了水面船的协同跟踪问题;Liu 等^[11-12]采用基于预估器的神经网络逼近不确定函数,取得了较好的效果,但是并未考虑海流干扰问题。

基于上述分析,对欠驱动 USV 受未知时变海流影响的研究较少,本文针对未知缓慢时变海流影响,提出了一种自适应海流观测器,并且采用神经网络逼近不确定函数,避免了因水动力学系数、速度等难以测定带来的困扰,通过采用动态面方法获取虚拟控制变量的导数,减少了直接求导的计算量,通过运用李雅普诺夫函数证明了该控制系统的稳定性,仿真验证了该控制器的有效性与鲁棒性。

1 问题描述

1.1 神经网络简述

RBF 神经网络能在一个紧凑集和任意精度下逼近任何非线性函数. 本文运用 RBF 神经网络逼近未知函数,RBF 神经网络算法为:

$$h_j = \exp\left(-\frac{\|\mathbf{x} - \mathbf{c}_j\|^2}{2b_j^2}\right),$$

$$\hat{f} = \mathbf{W}^* \mathbf{h}(\mathbf{x}) + \varepsilon_0.$$

式中: \mathbf{x} 为神经网络输入; i 为神经网络的输入个数; j 为神经网络隐含层第 j 个节点; $\mathbf{h} = [h_j]^T$ 为高斯函数的输出; \mathbf{W}^* 为神经网络的理想权值; μ 为神经网络的逼近误差;且 $\varepsilon_0 \leq \varepsilon_N$.

RBF 神经网络的输出为

$$\hat{f} = \mathbf{W}^T \mathbf{h}(\mathbf{x}).$$

式中: \hat{f} 为 f 的估计值, \mathbf{W} 神经网络的实际权值.

1.2 欠驱动 USV 运动坐标系

对于欠驱动 USV,设定固定坐标系为 $\{O_E, X_E, Y_E\}$,随体坐标系为 $\{O_B, X_B, Y_B\}$;对于 USV 而言,本

文只研究水平面内运动控制问题,USV 位姿及速度可表示为 $\{x, y, \psi\}$ 和 $\{u, v, r\}$,USV 轨迹跟踪如图 1 所示,期望运动轨迹为 $\eta_c(t)$,运动轨迹误差为 $\{x_e, y_e\}$.

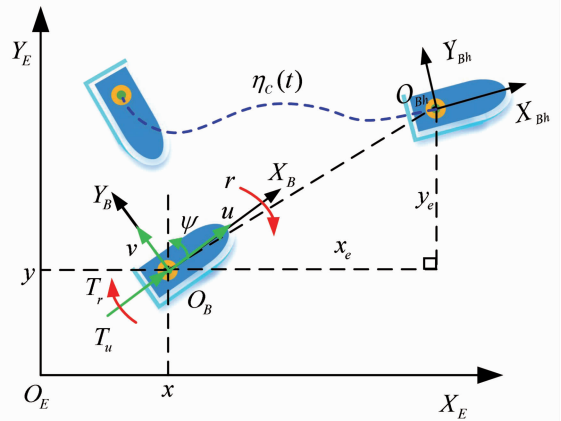


图 1 USV 水平面轨迹跟踪

Fig. 1 USV trajectory tracking on horizontal plane

1.3 欠驱动 USV 运动坐标系

对于欠驱动 USV,选取简化的 USV 运动数学方程和动力学方程为:

$$\dot{\boldsymbol{\eta}} = \mathbf{J}(\boldsymbol{\psi}) \mathbf{v} + \mathbf{v}_c, \quad (1)$$

$$\mathbf{M} \dot{\mathbf{v}} + \mathbf{C}(\mathbf{v}) \mathbf{v} + \mathbf{D} \mathbf{v} = \boldsymbol{\tau} + \mathbf{d}.$$

式中: $\boldsymbol{\eta} = [x \ y \ \psi]^T \in \mathbf{R}^3$ 为欠驱动 USV 惯性坐标系下的横坐标 x 、纵坐标 y 和偏航角 ψ 组成的向量; $\mathbf{v} = [u \ v \ r]^T \in \mathbf{R}^3$ 为欠驱动 USV 体坐标系下的横向速度 u 、纵向速度 v 和偏航角速度 r 组成的向量; $\mathbf{v}_c = [v_{cx} \ v_{cy} \ 0]^T \in \mathbf{R}^3$ 为欠驱动 USV 惯性坐标下的横向海流速度 v_{cx} 和纵向海流速度 v_{cy} 组成的向量; $\boldsymbol{\tau} = [\tau_u \ 0 \ \tau_r]^T \in \mathbf{R}^3$ 为欠驱动 USV 体坐标系下推力 τ_u 和偏转力矩 τ_r 组成的向量; $\mathbf{d} = [d_1 \ d_2 \ d_3]^T \in \mathbf{R}^3$ 为欠驱动 USV 体坐标系下受到的横向干扰力 d_1 、纵向干扰力 d_2 和偏航干扰力矩 d_3 组成的向量; $\mathbf{J}(\boldsymbol{\psi}) \in \mathbf{R}^{3 \times 3}$ 为坐标系转换矩阵,且满足 $\boldsymbol{\eta}_c = [x_c \ y_c \ \psi_c]^T$ 和 $\|\mathbf{J}(\boldsymbol{\psi})\| = 1$; $\mathbf{M} \in \mathbf{R}^{3 \times 3}$ 为欠驱动 USV 惯性质量和水动力附加惯性矩阵; $\mathbf{C}(\mathbf{v}) \in \mathbf{R}^{3 \times 3}$ 为科氏离心矩阵; $\mathbf{D} \in \mathbf{R}^{3 \times 3}$ 为非线性水动力阻尼矩阵.

$\mathbf{J}(\boldsymbol{\psi})$ 、 \mathbf{M} 和 \mathbf{D} 分别为:

$$\mathbf{J}(\boldsymbol{\psi}) = \begin{bmatrix} \cos \psi & -\sin \psi & 0 \\ \sin \psi & \cos \psi & 0 \\ 0 & 0 & 1 \end{bmatrix},$$

$$\mathbf{M} = \begin{bmatrix} m - X_u & 0 & 0 \\ 0 & m - Y_v & 0 \\ 0 & 0 & m - N_r \end{bmatrix} = \begin{bmatrix} m_{11} & 0 & 0 \\ 0 & m_{22} & 0 \\ 0 & 0 & m_{33} \end{bmatrix},$$

$$D = \begin{bmatrix} X_u + X_{u|u} |u| & 0 & 0 \\ 0 & Y_v + Y_{v|v} |v| & 0 \\ 0 & 0 & N_r + N_{r|r} |r| \end{bmatrix}.$$

式中: m_{11}, m_{22}, m_{33} 分别为欠驱动USV的惯性矩阵在船体坐标系上的3个分量; X_u, Y_v, N_r 分别为欠驱动USV阻尼矩阵在体坐标系上的3个分量; $X_{u|u}, Y_{v|v}, N_{r|r}$ 分别为欠驱动USV的非线性阻尼项。

2 控制器设计

2.1 建立轨迹跟踪误差方程

定义欠驱动USV在惯性坐标系下的期望位置和偏航角为 $\boldsymbol{\eta}_c = [x_c \ y_c \ \psi_c]^T$,则欠驱动USV在惯性坐标下的轨迹跟踪误差为:

$$x_e = x_c - x, y_e = y_c - y, \psi_e = \psi_c - \psi. \quad (2)$$

根据式(2),可得体坐标下轨迹跟踪误差为

$$\begin{cases} e_x = x_e \cos \psi + y_e \sin \psi, \\ e_y = -x_e \sin \psi + y_e \cos \psi, \\ e_\psi = \psi_e, \end{cases} \quad (3)$$

对式(3)求导,可得:

$$\begin{cases} \dot{e}_x = -u + v_m \cos \psi_e + re_y - v_{cx} \cos \psi - v_{cy} \sin \psi, \\ \dot{e}_y = -v + v_m \sin \psi_e - re_x + v_{cx} \sin \psi - v_{cy} \cos \psi, \\ \dot{e}_\psi = \dot{\psi}_e, \end{cases}$$

式中,期望合速度为 $v_m = \sqrt{\dot{x}_c^2 + \dot{y}_c^2}$.

2.2 稳定 e_x 和 e_y

定义一个李雅普诺夫函数为

$$V_1 = \frac{1}{2}(e_x^2 + e_y^2), \quad (4)$$

对式(4)求导,可得:

$$\begin{aligned} \dot{V}_1 = & e_x(-u + v_m \cos \psi_e + re_y - v_{cx} \cos \psi - v_{cy} \sin \psi) + \\ & e_y(-v + v_m \sin \psi_e + re_x + v_{cx} \sin \psi - v_{cy} \cos \psi). \end{aligned} \quad (5)$$

定义一个新的变量: $\kappa = v_m \sin \psi_e$.

为保证 \dot{V}_1 为负值,以 u 和 κ 为虚拟控制输入,选择其期望值为

$$\begin{cases} u_c = \alpha_1 e_x + v_m \cos \psi_e - \dot{v}_{cx} \cos \psi - \dot{v}_{cy} \sin \psi, \\ \kappa_c = -\alpha_2 e_y + v - \dot{v}_{cx} \sin \psi + \dot{v}_{cy} \cos \psi, \end{cases} \quad (6)$$

式中, $\alpha_1 > 0, \alpha_2 > 0$,且均为正实数。

将式(6)代入式(5),可得:

$$\dot{V}_1 = -\alpha_1 e_x^2 - \alpha_2 e_y^2 + \xi, \quad (7)$$

式中, $\xi = v_{cx}^e (e_y \sin \psi - e_x \cos \psi) - v_{cy}^e (e_x \sin \psi + e_y \cos \psi)$.

由于对虚拟控制变量直接求导较为复杂,为减小直接求导的复杂性,将 u_c, κ_c 和后文的 r_c 通过一阶滤波器,即

$$\begin{cases} \gamma_u \dot{u}_{cf}(t) + u_{cf}(t) = u_c(t), \\ \gamma_\kappa \dot{\kappa}_{cf}(t) + \kappa_{cf}(t) = \kappa_c(t), \\ \gamma_r \dot{r}_{cf}(t) + r_{cf}(t) = r_c(t), \end{cases}$$

其中初始值为:

$$u_{cf}(0) = u_c(0), \kappa_{cf}(0) = \kappa_c(0), r_{cf}(0) = r_c(0).$$

式中: u_{cf}, v_{cf}, r_{cf} 为虚拟控制变量通过一阶滤波器后的滤波值; $\gamma_u > 0, \gamma_\kappa > 0, \gamma_r > 0$ 且均为正实数。

2.3 稳定 e_u 和 z_u

定义欠驱动USV系统的速度误差变量:

$$e_u = u - u_{cf}, z_u = u_{cf} - u_c. \quad (8)$$

将式(8)代入方程(7),可得:

$$\dot{V}_1 = -\alpha_1 e_x^2 - \alpha_2 e_y^2 - e_u e_x + e_\kappa e_y + \xi.$$

定义一个新的李雅普诺夫函数为

$$V_2 = V_1 + \frac{1}{2}(e_u^2 + z_u^2), \quad (9)$$

对式(9)求导,可得:

$$\begin{aligned} \dot{V}_2 = & \dot{V}_1 + e_u \dot{e}_u + z_u \dot{z}_u = \\ & -\alpha_1 e_x^2 - \alpha_2 e_y^2 - e_u e_x + e_\kappa e_y + e_u \dot{e}_u + z_u \dot{z}_u + \xi = \\ & -\alpha_1 e_x^2 - \alpha_2 e_y^2 + e_u (\dot{e}_u - e_x) + e_\kappa e_y + z_u \dot{z}_u + \xi. \end{aligned}$$

2.4 稳定 e_ψ, e_κ 和 z_κ

定义欠驱动USV系统的速度误差变量:

$$e_\kappa = \kappa - \kappa_{cf}, z_\kappa = \kappa_{cf} - \kappa_c. \quad (10)$$

定义一个新的李雅普诺夫函数为

$$V_3 = V_2 + \frac{1}{2}(e_\psi^2 + e_\kappa^2 + z_\kappa^2), \quad (11)$$

对式(11)求导,可得:

$$\begin{aligned} \dot{V}_3 = & \dot{V}_2 + e_\psi \dot{e}_\psi + e_\kappa \dot{e}_\kappa + z_\kappa \dot{z}_\kappa = \\ & -\alpha_1 e_x^2 - \alpha_2 e_y^2 + e_u (\dot{e}_u - e_x) + z_u \dot{z}_u + z_\kappa \dot{z}_\kappa + \\ & e_\psi \dot{e}_\psi + e_\kappa \dot{e}_\kappa + e_\kappa e_y + \xi = -\alpha_1 e_x^2 - \alpha_2 e_y^2 + \\ & e_u (\dot{e}_u - e_x) + z_u \dot{z}_u + z_\kappa \dot{z}_\kappa + \xi + \\ & e_\psi \left[e_y + v_m \sin \psi_e + (v_m \cos \psi_e + \frac{e_\psi}{e_\kappa})(\dot{\psi}_d - r) - \dot{\kappa}_{cf} \right], \end{aligned} \quad (12)$$

式中 r 为虚拟控制变量。

可设定 r 的期望值为

$$r_c = -\alpha_3 e_\kappa + \dot{\psi}_c + \frac{e_y + v_m \sin \psi_e - \kappa_{cf}}{v_m \cos \psi_e + e_\psi / e_\kappa}, \quad (13)$$

式中, $\alpha_3 > 0$,且为正实数。

将式(13)代入式(12),可得:

$$\begin{aligned} \dot{V}_3 = & -\alpha_1 e_x^2 - \alpha_2 e_y^2 - \alpha_3 e_\kappa^2 + e_u (\dot{e}_u - e_x) + \\ & z_u \dot{z}_u + z_\kappa \dot{z}_\kappa + \xi. \end{aligned} \quad (14)$$

2.5 稳定 e_r 和 z_r

定义速度误差变量为:

$$e_r = r - r_{cf}, z_r = r_{cf} - r_c, \quad (15)$$

将式(15)代入式(14),可得:

$$\dot{V}_3 = -\alpha_1 e_x^2 - \alpha_2 e_y^2 - \alpha_3 e_\kappa^2 + e_u (\dot{e}_u - e_x) - v_m e_\kappa e_r \cos \psi_e + z_u \dot{z}_u + z_\kappa \dot{z}_\kappa + \xi.$$

定义一个新的李雅普诺夫函数为

$$V_4 = V_3 + \frac{1}{2}(e_r^2 + z_r^2), \quad (16)$$

对式(16)求导,可得:

$$\begin{aligned} \dot{V}_4 = \dot{V}_3 + e_r \dot{e}_r + z_r \dot{z}_r = & -\alpha_1 e_x^2 - \alpha_2 e_y^2 - \alpha_3 e_\kappa^2 + \\ & e_u (\dot{e}_u - e_x) + e_r (\dot{e}_r - v_m e_\kappa e_r \cos \psi_e) + \\ & z_u \dot{z}_u + z_\kappa \dot{z}_\kappa + z_r \dot{z}_r + \xi. \end{aligned} \quad (17)$$

2.6 控制输入设计

由于欠驱动 USV 速度难以准确测定以及水动力学系数难以确定,此处定义不确定函数:

$$\begin{cases} \vartheta_1 = m_{22}vr - X_u u - X_{u|u}|u|, \\ \vartheta_3 = (m_{11} - m_{22})uw - N_r r - N_{r|r}|r|. \end{cases}$$

针对不确定函数,采用神经网络进行逼近,定义神经网络预测误差为:

$$\hat{\delta}_1 = \vartheta_1 - \hat{\vartheta}_1, \hat{\delta}_3 = \vartheta_3 - \hat{\vartheta}_3. \quad (18)$$

选取控制输入为

$$\begin{cases} \tau_u = -m_{11}(\beta_1 e_u + e_x + \dot{u}_{cf}) + \hat{W}_1 h(\mathbf{x}_u) + \\ \quad \delta_1 \sigma_1 + \eta_1 \operatorname{sgn}(e_u), \\ \tau_r = -m_{33}(\beta_3 e_r + e_\kappa v_m \cos \psi_e + \dot{r}_{cf}) + \hat{W}_3 h(\mathbf{x}_r) + \\ \quad \delta_3 \sigma_3 + \eta_3 \operatorname{sgn}(e_r). \end{cases} \quad (19)$$

式中: \hat{W}_1, \hat{W}_3 分别为神经网络权值 W_1 和 W_3 的估计值; $\beta_1 > 0, \sigma_1 > 0, \eta_1 > 0, \beta_3 > 0, \sigma_3 > 0, \eta_3 > 0$ 均为正实数.

选取自适应律为

$$\begin{cases} \dot{\hat{W}}_1 = \chi_1 [(e_u + \lambda_1 \delta_1)h(\mathbf{x}_u) - \rho_1 \hat{W}_1], \\ \dot{\hat{W}}_3 = \chi_3 [(e_r + \lambda_3 \delta_3)h(\mathbf{x}_r) - \rho_3 \hat{W}_3], \end{cases} \quad (20)$$

式中, $\chi_1 > 0, \chi_3 > 0$ 均为正实数.

将式(1)代入式(19),可得:

$$\begin{cases} m_{11} \dot{e}_u = -m_{11}(\beta_1 e_u + e_x + \dot{u}_{cf}) + \\ \quad \hat{W}_1 h(\mathbf{x}_u) - \vartheta_1 + d_1 - \eta_1 \operatorname{sgn}(e_u), \\ m_{33} \dot{e}_r = -m_{33}(\beta_3 e_r + e_\kappa v_m \cos \psi_e + \dot{r}_{cf}) + \\ \quad \hat{W}_3 h(\mathbf{x}_r) - \vartheta_3 + d_3 - \eta_3 \operatorname{sgn}(e_r). \end{cases} \quad (21)$$

将式(21)代入式(17),可得:

$$\begin{aligned} \dot{V}_4 = & -\alpha_1 e_x^2 - \alpha_2 e_y^2 - \alpha_3 e_\kappa^2 - \beta_1 e_u^2 - \beta_3 e_r^2 + \\ & \hat{W}_1 h(\mathbf{x}_u) e_u - m_{11}(\eta_1 |e_u| - d_1 e_u) + \\ & \hat{W}_3 h(\mathbf{x}_r) e_r - m_{33}(\eta_3 |e_r| - d_3 e_r) + \\ & z_u \dot{z}_u + z_\kappa \dot{z}_\kappa + z_r \dot{z}_r + \xi, \end{aligned} \quad (22)$$

式中, \tilde{W}_1, \tilde{W}_3 分别为神经网络权值 W_1 和 W_3 的估计误差,且有 $\tilde{W}_1 = \hat{W}_1 - W_1^*, \tilde{W}_3 = \hat{W}_3 - W_3^*$.

假设 1 对所有神经网络理想权值矩阵 W^* 和逼近误差 ε 有界,即存在正常数 W_M 和有界函数 ε_M ,使得 $\|W^*\| \leq W_M$ 和 $\|\varepsilon\| \leq \varepsilon_M$.

2.7 海流观测器设计

针对海洋环境中未知时变海流,本文设计了一种指数收敛自适应观测器,目标为海流估计值指数趋近于未知时变海流,即

$$\dot{\hat{v}}_c = \dot{\eta} - J(\psi)v. \quad (23)$$

对于设计的海流观测器,可以选择:

$$\dot{\hat{v}}_c = -\hat{K}v_c + K\dot{\eta} - KJ(\psi)v. \quad (24)$$

式中: $\hat{v}_c = [\hat{v}_{cx} \quad \hat{v}_{cy} \quad 0]^T \in \mathbf{R}^3$ 为海流观测器对未知海流的估计向量; $K = \operatorname{diag}[k_1 \quad k_2 \quad 0] \in \mathbf{R}^{3 \times 3}$ 为待定的正定参数对角阵向量.

将式(24)代入式(23),可得:

$$\dot{v}_c^e = \dot{\hat{v}}_c - \dot{v} = \hat{K}v_c - K\dot{\eta} + KJ(\psi)v = -Kv_c^e, \quad (25)$$

式中, $v_c^e = [v_{cx}^e \quad v_{cy}^e \quad 0]^T \in \mathbf{R}^3$ 为海流观测器观测误差组成的向量.

根据式(25)可知,设计的未知海流观测器是指数稳定的;但是,在欠驱动 USV 实际航行过程中,惯性坐标系下的速度 $\dot{\eta}$ 是难以测定的变量;此时,引入辅助变量 ζ 为 $\zeta = \hat{v}_c - K\dot{\eta}$,选取: $\dot{\zeta} = -K\zeta + K(-K - J(\psi)v)$,则有

$$\begin{aligned} \dot{v}_c^e = \dot{\hat{v}}_c - \dot{v} = & -\dot{\zeta} - K\dot{\eta} = \\ & K\zeta - K(-K\dot{\eta} - J(\psi)v) - K\dot{\eta} = \\ & K(\hat{v}_c - v_c) = -Kv_c^e. \end{aligned}$$

综上所述,设计的海流观测器是指数收敛的.

3 稳定性分析

为稳定欠驱动 USV 轨迹跟踪控制器与海流观测器所组成的闭环系统,将整个控制系统分解为两个子系统.

定义第 1 个子系统 Σ_1 为

$$\|x_1\| = [e_x \quad e_y \quad e_\psi \quad e_u \quad e_\kappa \quad e_r \quad \tilde{W}_1 \quad \tilde{W}_3 \quad \delta_1 \quad \delta_3].$$

根据文献[13]可得:

$$\begin{cases} \dot{z}_u = \dot{u}_{cf} - \dot{u}_c = -z_u/\gamma_u + du_c/dt, \\ |du_c/dt| \leq \zeta_u, \end{cases} \quad (26)$$

式中, $\zeta_u > 0$,且为正实数.

将式(10)代入式(26),可得:

$$z_u \dot{z}_u \leq -\frac{z_u^2}{\gamma_u} + \zeta_u |\zeta_u| \leq -\frac{z_u^2}{\gamma_u} + z_u^2 + \frac{1}{4}\zeta_u^2. \quad (27)$$

将不等式(27)代入式(22), 可得:

$$\begin{aligned} \dot{V}_4 \leq & -\alpha_1 e_x^2 - \alpha_2 e_y^2 - \alpha_3 e_\kappa^2 - \beta_1 e_u^2 - \beta_3 e_r^2 + \\ & \tilde{W}_1^T h(\mathbf{x}_u) e_u - m_{11}(\eta_1 |e_u| - d_1 e_u) + \\ & \tilde{W}_3^T h(\mathbf{x}_r) e_r - m_{33}(\eta_3 |e_r| - d_3 e_r) - \\ & \left(1 - \frac{1}{\gamma_u}\right) z_u^2 - \left(1 - \frac{1}{\gamma_\kappa}\right) z_\kappa^2 - \left(1 - \frac{1}{\gamma_r}\right) z_r^2 + \\ & \frac{1}{4}(\zeta_u^2 + \zeta_\kappa^2 + \zeta_r^2). \end{aligned}$$

式中, $\zeta_\kappa > 0, \zeta_r > 0$, 且均为正实数.

根据式(18), 可得:

$$\dot{\delta}_i = \vartheta_i - \hat{\vartheta}_i = \tilde{W}_i^T h(\mathbf{x}) + \varepsilon_i - \sigma_i \delta_i, (i=1,3) \quad (28)$$

式中, $\varepsilon_1 > 0, \varepsilon_3 > 0$, 均为待定的正实数.

根据式(28), 可得:

$$\delta_i \dot{\delta}_i = \delta_i \tilde{W}_i^T h(\mathbf{x}) + \delta_i \varepsilon_i - \sigma_i \delta_i^2, (i=1,3).$$

定义一个新的李雅普诺夫函数:

$$\begin{aligned} V_5 = & V_4 + \frac{1}{2\chi_1} \tilde{W}_1^T \tilde{W}_1 + \frac{1}{2\chi_3} \tilde{W}_3^T \tilde{W}_3 + \\ & \frac{1}{2} \lambda_1 \delta_1^2 + \frac{1}{2} \lambda_3 \delta_3^2, \end{aligned} \quad (29)$$

对式(29)求导, 可得:

$$\begin{aligned} \dot{V}_5 = & \dot{V}_4 - \frac{1}{\chi_1} \tilde{W}_1^T \dot{\tilde{W}}_1 - \frac{1}{\chi_3} \tilde{W}_3^T \dot{\tilde{W}}_3 + \lambda_1 \delta_1 \dot{\delta}_1 + \lambda_3 \delta_3 \dot{\delta}_3 = \\ & \dot{V}_4 - \tilde{W}_1^T h(\mathbf{x}_u) (e_u + \lambda_1 \delta_1) + \rho_1 \tilde{W}_1^T \hat{W}_1 - \\ & \tilde{W}_3^T h(\mathbf{x}_r) (e_r + \lambda_3 \delta_3) + \rho_3 \tilde{W}_3^T \hat{W}_3 + \\ & \lambda_1 \delta_1 \tilde{W}_1^T h(\mathbf{x}_u) + \lambda_1 \delta_1 \varepsilon_1 - \lambda_1 \sigma_1 \delta_1^2 + \\ & \lambda_3 \delta_3 \tilde{W}_3^T h(\mathbf{x}_r) + \lambda_3 \delta_3 \varepsilon_3 - \lambda_3 \sigma_3 \delta_3^2. \end{aligned} \quad (30)$$

将式(20)代入式(30), 可得:

$$\begin{aligned} \dot{V}_5 \leq & -\alpha_1 e_x^2 - \alpha_2 e_y^2 - \alpha_3 e_\kappa^2 - \beta_1 e_u^2 - \beta_3 e_r^2 - \\ & m_{11}(\eta_1 |e_u| - d_1 e_u) - m_{33}(\eta_3 |e_r| - d_3 e_r) - \\ & \rho_1 \tilde{W}_1^T \tilde{W}_1 + \rho_1 \tilde{W}_1^T \mathbf{W}_1^* + \lambda_1 \delta_1 \varepsilon_1 - \lambda_1 \sigma_1 \delta_1^2 - \\ & \rho_3 \tilde{W}_3^T \tilde{W}_3 + \rho_3 \tilde{W}_3^T \mathbf{W}_3^* + \lambda_3 \delta_3 \varepsilon_3 - \lambda_3 \sigma_3 \delta_3^2 - \\ & \left(1 - \frac{1}{\gamma_u}\right) z_u^2 - \left(1 - \frac{1}{\gamma_\kappa}\right) z_\kappa^2 - \left(1 - \frac{1}{\gamma_r}\right) z_r^2 + \\ & \frac{1}{4}(\zeta_u^2 + \zeta_\kappa^2 + \zeta_r^2). \end{aligned} \quad (31)$$

根据文献[14], 可得以下方程:

$$\begin{cases} \delta_i \varepsilon_i - \sigma_i \delta_i^2 = -\sigma_i \left(\delta_i - \frac{\varepsilon_i}{2\sigma_i}\right)^2 + \frac{1}{4\sigma_i} \varepsilon_i^2, (i=1,3) \\ \tilde{W}_i^T \mathbf{W}_i^* - \tilde{W}_i^T \tilde{W}_i = -\left\| \tilde{W}_i - \frac{\mathbf{W}_i^*}{2} \right\|^2 + \\ \frac{1}{4} \left\| \mathbf{W}_i^* \right\|^2, (i=1,3) \end{cases} \quad (32)$$

将式(32)代入式(31), 可得:

$$\begin{aligned} \dot{V}_5 \leq & -\alpha_1 e_x^2 - \alpha_2 e_y^2 - \alpha_3 e_\kappa^2 - \alpha_4 e_u^2 - \alpha_5 e_r^2 - \\ & m_{11}(\eta_1 |e_u| - d_1 e_u) - m_{33}(\eta_3 |e_r| - d_3 e_r) - \\ & \rho_1 \left[\left\| \tilde{W}_1 - \frac{\mathbf{W}_1^*}{2} \right\|^2 - \frac{1}{4} \left\| \mathbf{W}_1^* \right\|^2 \right]^2 - \\ & \lambda_1 \left[\sigma_1 \left(\delta_1 - \frac{\varepsilon_1}{2\sigma_1} \right)^2 - \frac{1}{4\sigma_1} \varepsilon_1^2 \right]^2 - \\ & \rho_3 \left[\left\| \tilde{W}_3 - \frac{\mathbf{W}_3^*}{2} \right\|^2 - \frac{1}{4} \left\| \mathbf{W}_3^* \right\|^2 \right]^2 - \\ & \lambda_3 \left[\sigma_3 \left(\delta_3 - \frac{\varepsilon_3}{2\sigma_3} \right)^2 - \frac{1}{4\sigma_3} \varepsilon_3^2 \right]^2 - \\ & \left(1 - \frac{1}{\gamma_u}\right) z_u^2 - \left(1 - \frac{1}{\gamma_\kappa}\right) z_\kappa^2 - \left(1 - \frac{1}{\gamma_r}\right) z_r^2 + \\ & \frac{1}{4}(\zeta_u^2 + \zeta_\kappa^2 + \zeta_r^2) \leq -\alpha_1 e_x^2 - \alpha_2 e_y^2 - \alpha_3 e_\kappa^2 - \\ & \alpha_4 e_u^2 - \alpha_5 e_r^2 - m_{11}(\eta_1 |e_u| - d_1 e_u) - \\ & m_{33}(\eta_3 |e_r| - d_3 e_r) - \\ & \min \sigma_{\min} \left[\left(\delta_1 - \frac{\varepsilon_1}{2\sigma_1} \right)^2 + \left(\delta_3 - \frac{\varepsilon_3}{2\sigma_3} \right)^2 \right] - \\ & \lambda \rho_{\min} \left[\left\| \tilde{W}_1 - \frac{\mathbf{W}_1^*}{2} \right\|^2 + \left\| \tilde{W}_3 - \frac{\mathbf{W}_3^*}{2} \right\|^2 \right] + \Theta. \end{aligned} \quad (33)$$

式中: $\lambda_{\min} = \min\{\lambda_1, \lambda_3\}$, $\sigma_{\min} = \min\{\sigma_1, \sigma_3\}$, $\rho_{\min} = \min\{\rho_1, \rho_3\}$, $\Theta = \frac{\lambda_{\max}}{2\sigma_{\min}} \varepsilon_M^2 + \frac{\rho_{\max}}{2} W_M^2$, $\lambda_{\max} = \max\{\lambda_1, \lambda_3\}$, $\rho_{\max} = \max\{\rho_1, \rho_3\}$.

根据式(33)可知, 通过选取不同的控制器参数, 可保证 $\dot{V}_5 \leq 0$, 即子系统 \sum_1 是收敛的.

定义第 2 个子系统 \sum_2 为

$$\| \mathbf{x}_2 \| = [v_{cx}^e \ v_{cy}^e].$$

定义一个新的李雅普诺夫函数为

$$V_6 = \frac{1}{2}((v_{cx}^e)^2 + (v_{cy}^e)^2), \quad (34)$$

对式(34)求导, 可得:

$$\dot{V}_6 = v_{cx}^e \dot{v}_{cx}^e + v_{cy}^e \dot{v}_{cy}^e = -k_1 (v_{cx}^e)^2 - k_2 (v_{cy}^e)^2,$$

则子系统 \sum_2 为指数稳定的.

定义一个新的李雅普诺夫函数为

$$V = V_5 + V_6,$$

则 \dot{V} 可进一步表示为

$$\dot{V} \leq -2\mu V + \Phi, \quad (35)$$

式中, μ, Φ 分别为:

$$\begin{aligned} \mu = & \min\{\alpha_1, \alpha_2, \alpha_3, \alpha_4, \alpha_5, \rho_1, \lambda_1, \rho_3, \lambda_3, \\ & (1 - \frac{1}{\gamma_u}), (1 - \frac{1}{\gamma_\kappa}), (1 - \frac{1}{\gamma_r}), k_1, k_2\}, \\ \Phi = & \frac{1}{4}(\zeta_u^2 + \zeta_\kappa^2 + \zeta_r^2) + \frac{\lambda_{\max}}{2\sigma_{\min}} \varepsilon_M^2 + \frac{\rho_{\max}}{2} W_M^2. \end{aligned}$$

对式(35)求解可得:

$$V \leq \frac{\Phi}{2\mu} + \left[V(0) - \frac{\Phi}{2\mu} \right] e^{-2\mu t}.$$

显然,当 $t \rightarrow \infty$ 时,有 $V \rightarrow \Phi/2\mu$,则闭环系统的所有信号是半全局一致最终有界的,即所设计的控制器是稳定的.

4 仿真分析

本文选取文献[15]欠驱动 USV 系统模型和外界干扰,验证文中设计的控制算法,取欠驱动 USV 初始条件为:

$$\eta(0) = [0 \quad 17 \quad 0]^T, \nu(0) = [0.4 \quad 0 \quad 0]^T.$$

欠驱动 USV 应用过程中, τ_u, τ_r 是有限的,在控制器设计中,设定控制输入为有限值,即

$$0 \leq |\tau_u| \leq 90 \text{ N}, 0 \leq |\tau_r| \leq 20 \text{ N} \cdot \text{m}.$$

控制器参数为: $\alpha_1 = 0.5, \alpha_2 = 0.4, \alpha_3 = 0.3, \alpha_4 = 0.2, \alpha_5 = 1.0, \gamma_u = 0.1, \gamma_\kappa = 0.1, \gamma_r = 0.1, \eta_1 = 0.2, \eta_3 = 0.2, \chi_1 = 0.1, \chi_3 = 0.1, \lambda_1 = 0.15, \lambda_3 = 0.10, \rho_1 = 0.3, \rho_3 = 0.2$,神经网络的初始权值取 $0.1, c_j = [-1.0 \quad -0.5 \quad 0 \quad 0.5 \quad 1.0]$ 和 $b_j = 5.0$.

缓慢变化海流选取为

$$\begin{cases} v_{cx} = (-0.1 - 0.1 \sin(0.01t)), \\ v_{cy} = (-0.1 - 0.1 \cos(0.01t)). \end{cases}$$

为验证该控制器控制性能,选取预期圆轨迹为

$$\begin{cases} x_c(t) = 15 \sin(0.05t), \\ y_c(t) = 15 \cos(0.05t). \end{cases}$$

为便于仿真结果分析,仿真时间为 200 s,可清晰地看出运动轨迹,仿真结果如图 2 ~ 图 7 所示.

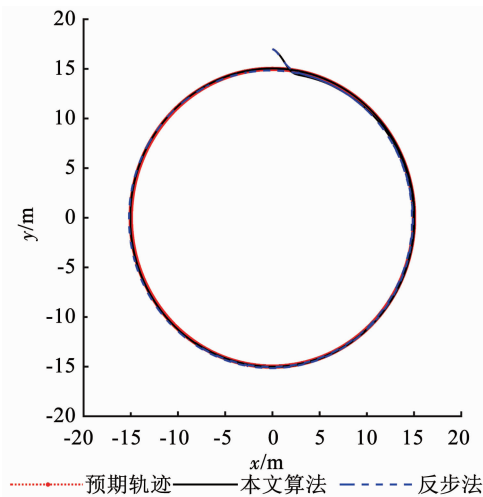


图 2 预期轨迹与实际运动轨迹

Fig. 2 Desired trajectory and actual trajectory

根据图 2 可知,在欠驱动 USV 航行初始阶段受海流影响较大,但在较短时间内有效地实现了轨迹跟踪;根据图 3、4 可得出,位置跟踪误差、速度跟踪误差均收敛到零附近的一个区域内;根据图 5 可知,

设计的神经网络自适应模型可有效逼近欠驱动 USV 系统未知函数;根据图 6 可知,设计的自适应海流观测器可有效观测未知缓慢时变海流. 根据图 7

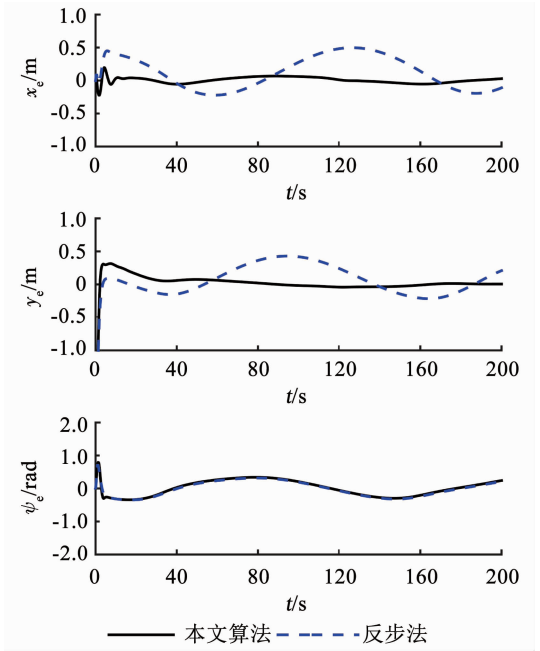


图 3 位置跟踪误差与偏航误差

Fig. 3 Position tracking errors and yaw errors

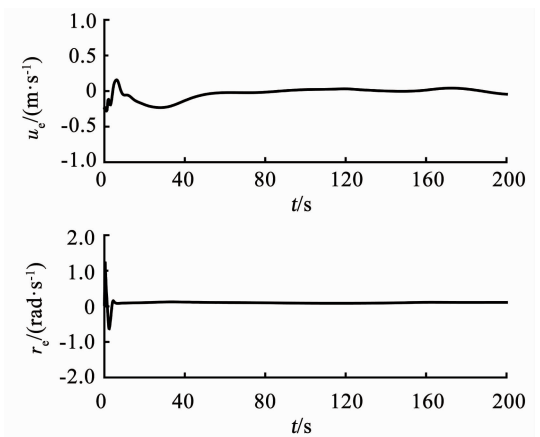


图 4 速度跟踪误差

Fig. 4 Velocity tracking errors

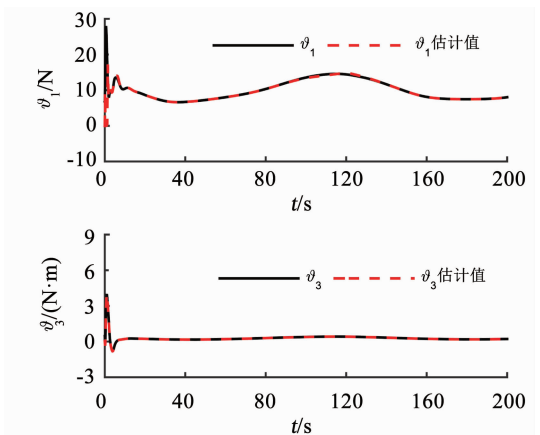


图 5 函数逼近误差

Fig. 5 Function approximation errors

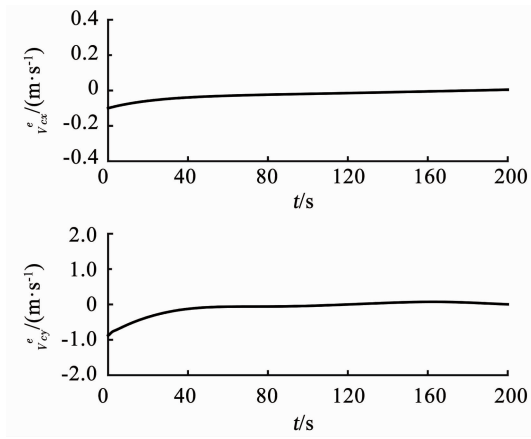


图6 海流速度观测误差

Fig. 6 Current velocity observation errors

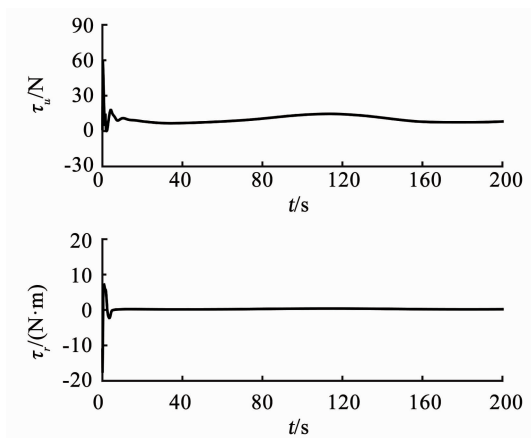


图7 控制力与控制力矩

Fig. 7 Control force and control moment

可知,控制力及控制力矩较为稳定,且在设定范围内。

5 结论

1)设计了一种自适应海流观测器,有效地估计了未知缓慢时变海流。

2)运用李雅普诺夫稳定性理论验证了欠驱动USV闭环控制系统的稳定性。

3)仿真结果表明,欠驱动USV轨迹跟踪误差、速度跟踪误差均收敛到零附近的一个区域内,验证了该控制系统的有效性。

参考文献

- [1]沈智鹏,张晓玲,张宁,等.基于神经网络观测器的船舶轨迹跟踪递归滑模动态面输出反馈控制[J].控制理论与应用,2018,35(8):1092
SHEN Zhipeng, ZHANG Xiaoling, ZHANG Ning, et al. Recursive sliding mode dynamic surface output feedback control for ship trajectory tracking based on neural network observer[J]. Control Theory & Applications, 2018, 35(8): 1092. DOI:10.7641/CTA.2018.70456
- [2]杜佳璐,杨杨,胡鑫,等.基于动态面控制的船舶动力定位控制律设计[J].交通运输工程,2014,14(5):362
DU Jialu, YANG Yang, HU Xin, et al. Control law design of

- dynamic positioning for ship based on dynamic surface control[J]. Journal of Traffic and Transportation Engineering, 2014, 14(5): 362. DOI:10.3969/j.issn.1671-1637.2014.05.005
- [3]张天平,施泉铖,沈启坤,等.具有未建模动态的自适应神经网络动态面控制[J].控制理论与应用,2013,30(4):475
ZHANG Tianping, SHI Xiaocheng, SHEN Qikun, et al. Adaptive neural-network dynamic surface-control with unmodeled dynamics[J]. Control Theory & Applications, 2013, 30(4): 475. DOI:10.7641/CTA.2013.21022
- [4]廖煜雷,万磊,庄佳园.欠驱动船路径跟踪的反演自适应动态滑模控制方法[J].中南大学学报(自然科学版),2012,43(7):2655
LIAO Yulei, WAN Lei, ZHUANG Jiayuan. Backstepping adaptive dynamical sliding mode control method for path following of underactuated surface vessel[J]. Journal of Central South University (Science and Technology), 2012, 43(7): 2655
- [5]王金强,王聪,魏英杰,等.未知海流干扰下自主水下航行器位置跟踪控制策略研究[J].兵工学报,2019,40(3):583
WANG Jinqiang, WANG Cong, WEI Yingjie, et al. Position tracking control of autonomous underwater vehicles in the disturbance of unknown ocean currents[J]. Acta Armamentarii, 2019, 40(3): 583. DOI:10.3969/j.issn.1000-1093.2019.03.018
- [6]TEEK P, GE S S. Control of fully actuated ocean surface vessels using a class of feedforward approximators[J]. IEEE Transactions on Control Systems Technology, 2006, 14(4): 750. DOI:10.1109/tcst.2006.872507
- [7]SHOJAEI K. Observer-based neural adaptive formation control of autonomous surface vessels with limited torque[J]. Robotics and Autonomous Systems, 2016, 78(C): 83. DOI:10.1016/j.robot.2016.01.005
- [8]WANG Jinqiang, WANG Cong, WEI Yingjie, et al. Three-dimensional path following of an underactuated AUV based on neuro-adaptive command filtered backstepping control[J]. IEEE Access, 2018, 6: 74355. DOI:10.1109/ACCESS.2018.2883081
- [9]PAN Changzhong, LAI Xuzhi, YANG S X, et al. A bioinspired neural dynamics-based approach to tracking control of autonomous surface vehicles subject to unknown ocean currents[J]. Neural Computing and Applications, 2015, 26(8): 1929. DOI:10.1007/s00521-015-1839-6
- [10]WANG Hao, WANG Dan, PENG Zhouhua. Neural network based adaptive dynamic surface control for cooperative path following of marine surface vehicles via state and output feedback[J]. Neurocomputing, 2014, 133: 170. DOI:10.1016/j.neucom.2013.11.019
- [11]LIU Lu, WANG Dan, PENG Zhouhua. Path following of marine surface vehicles with dynamical uncertainty and time-varying ocean disturbances[J]. Neurocomputing, 2016, 173: 799. DOI:10.1016/j.neucom.2015.08.033
- [12]LIU Lu, WANG Dan, PENG Zhouhua. Direct and composite iterative neural control for cooperative dynamic positioning of marine surface vessels[J]. Nonlinear Dynamics, 2015, 81: 1315. DOI:10.1007/s11071-015-2071-8
- [13]SHOJAEI K, DOLATSHAHI M. Line-of-sight target tracking control of underactuated autonomous underwater vehicles[J]. Ocean Engineering, 2017, 133: 244. DOI:10.1016/j.oceaneng.2017.02.007
- [14]XU Bin, SHI Zhongke, YANG Chenguang, et al. Composite neural dynamic surface control of a class of uncertain nonlinear systems in strict-feedback form[J]. IEEE Transactions on Cybernetics, 2014, 44(12): 2626. DOI:10.1109/TCYB.2014.2311824
- [15]DO K D, PAN J. Robust path-following of underactuated ships: Theory and experiments on a model ship[J]. Ocean Engineering, 2006, 33(10): 1354. DOI:10.1016/j.oceaneng.2005.07.011